Journal of Engineering Science and Technology
Vol. 14, No. 2 (2019) 1088 - 1100

DESIGN OPTIMIZATION OF MULTI-KINK AXIAL RADIAL DIFFUSER OF STEAM TURBINE EXHAUST HOODS

VEERABATHRASWAMY KANDASAMY, SENTHIL KUMAR ARUMUGAM*

CO_2 Research and Green Technologies Centre, Vellore Institute of Technology,
Vellore, Tamil Nadu, India - 632 014
*Corresponding Author: asenthilkumar@vit.ac.in

Abstract

A new procedure to design the multi-kink axial radial diffuser of a steam turbine exhaust hood has been developed. In phase 1, the sensitivity of the parameters, which define the exhaust hood outer boundary - the end-wall distance from the turbine exit and the outer casing diameter and the effect of having a volute casing as well have been studied to arrive at a better design envelope. For this design envelope, design optimization of a multi-kink axial radial diffuser has been carried out using the Design of Experiments in phase 2. The compressible 3D Navier-Stokes equations with standard k-ε turbulence model has been solved. The results reveal that there exists a minimum end-wall distance below, which flow separations occur. Besides the end-wall distance, the gap between the outlet of the diffuser and the outer casing is found to be another significant parameter in influencing the performance. A right combination of diffuser tip geometrical parameters has been arrived at to produce an enhanced performance.

Keywords: CFD; Diffuser design optimization; Multi-kink diffuser design, Steam turbine exhaust hood performance.

1. Introduction

Steam turbines, the preferred thermal energy conversion devices for the base load power plants, are typically built for large capacities in the tune of 1000 MW. Due to the large capacity, every small improvement in the energy conversion efficiency has significant cost saving benefits. Of various components, the exhaust hood, which has still room for improvement, has been the focus of research in recent years [1]. The exhaust hood, which connects the turbine to the condenser converts a portion of the turbine outlet kinetic energy into pressure energy enabling to maintain a lower turbine exit pressure [2]. An exhaust hood consists of two regions: an axial-radial diffuser and a duct.

Design of an exhaust hood poses challenges as the flow turns by 90 degrees from a circular annulus cross section at the inlet to a square cross section at the outlet. The key performance requirements of an exhaust hood are lowering the turbine exit pressure, minimizing the total pressure loss and maximizing the flow uniformity at the turbine exit.

CFD analysis of an exhaust hood is a challenge due to a strong interaction that exists between the turbine stage and the exhaust hood. On the other hand, CFD simulations of the entire turbine and exhaust hood, which can predict the most accurate results, is computationally demanding. Hence, researchers have come up with a range of methods to couple the last stage turbine blades to capture the interaction [1]. Even these techniques such as mixing plane method, frozen rotor technique and actuator disk model are not preferred during the design process of an exhaust hood as it involves multiple iterations. Tindell et al. [2] simulated the performance of an exhaust hood using experimentally obtained inlet boundary conditions. The challenges associated with this reduced computational model in choosing the appropriate boundary conditions and turbulence model have been addressed by the authors in their previous work [3].

To achieve an optimized geometry, a good understanding of the influence of the geometrical parameters on the flow behaviour is required. Various researchers have attempted to understand the flow physics and performance of exhaust hood with experimental and CFD techniques [4-8]. Fan et al. [9] optimized the aerodynamic performance of a low-pressure exhaust system by the orthogonal experiments technique. Cao and You [10] attempted the improvement of the pressure recovery capability of an exhaust hood by diffuser shape optimization. Artificial neural network based intelligent algorithm [11] was attempted in the performance optimization by controlling the working conditions of the exhaust hood. Cao et al. [12] in their work on predicting the optimum flow guide tilt angle used a single variable approach. Cao et al. [13] reported the system level multi variable design optimization, in which, the presence of extraction pipe and boiler feed pump were considered. Verstraete et al. [14], in his work, used a meta model based evolution algorithm to optimize the diffuser tip curve. Fu et al. [15] reported that a coupled turbine stage and exhaust hood CFD model based optimization is.

The above described optimization methods focused on optimizing the diffuser geometry with smooth tip profiles. However, no literature reports the optimization of a multi-kink diffuser [16], which is preferred over a smooth curved diffuser due to its simplicity in construction. In addition to its simplicity, multi-kink diffusers are preferred by the industry as they have fixed separation points, which help in avoiding the unsteady separation. In addition to the diffuser geometry, other

geometrical parameters of the exhaust hood - the end-wall distance from the turbine exit, the outer diameter of the hood and the volute are critical to the performance.

This paper focuses on optimization of a multi-kink diffuser. This work has been conducted in two phases. In the first phase, the sensitivity of the parameters, which define the envelope of the exhaust hood- the end-wall distance and the outer diameter and the volute have been investigated to arrive at a better design envelope. In the second phase, firstly, a new procedure has been developed for the design of a multi-kink diffuser with eight variables. Then, optimization of the diffuser geometry has been carried out using the Design of Experiments.

2. Computational Model

An exhaust hood of a 300 MW steam turbine power plant is considered as the reference case. The trailing edge of the last stage turbine is considered as the inlet of the computational model and the outlet is defined at the condenser inlet. The computational domain of the exhaust hood is shown in Fig. 1 with an extended outlet plane for computational stability [3].

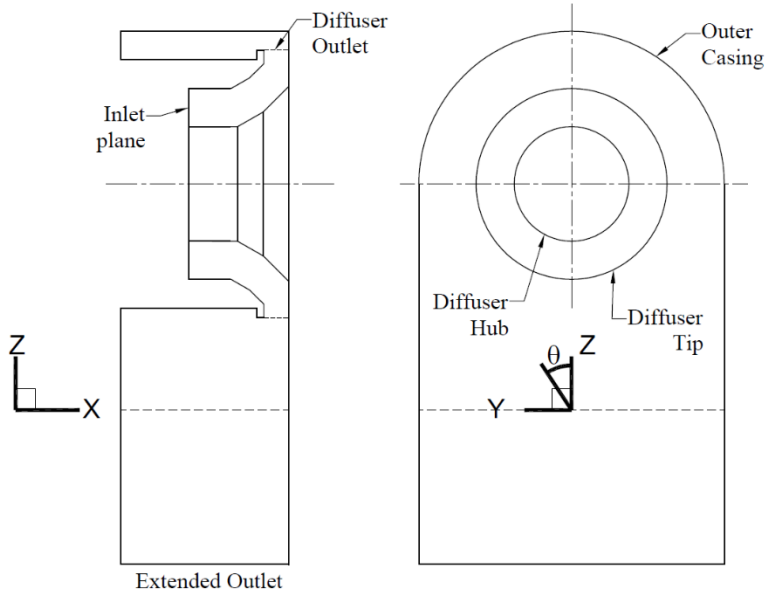

Fig. 1. Computational domain for exhaust hood flow analysis.

A complete hexahedral mesh is generated for this study using the multi-block approach with the help of commercial CFD mesh generation software, ICEMCFD HEXA. The inlet boundary is defined with 'total pressure' and it allows the variation of static pressure in the circumferential direction at the inlet plane. The outlet is specified with average static pressure. The summary of the boundary conditions used for this analysis is reported in Table 1.

Based on studies by Liu et al. [5], Compared to the model of a mesh of 120 × 70×41 grid points in, Z (axial), R (radial), directions is used in the base case, which is marginally a finer mesh. Two tests are conducted to check the grid independency

of the solution with a grid refinement factor of 1.3. The maximum variation in the predicted pressure loss is less than 3% and that of the pressure coefficient is less than 5% for all the three cases. In addition, when compared between the tests 2 and 3, the difference in the predicted pressure loss and recovery are less than 1%. Hence, the present grid of 120×70×41 is sufficient to resolve a grid independent solution.

A 3D, turbulent, viscous and compressible flow is solved by applying the Reynolds averaged Navier-Stokes equations using ANSYS FLUENT [17-19]. The authors in their previous work [3] have demonstrated the standard k-ε turbulence model predicts the flow behaviour to the required level of accuracy by validating with experimental data. In addition, the use of standard k-ε turbulence model requires much lower mesh count compared to the advanced turbulence models.

Major assumptions made in this analysis are as follows:

- The flow is steady.
- The flow is adiabatic at the solid wall.
- The obstruction for flow due to the furniture inside the hood will have no interaction effect with the considered design variables. Hence, furniture effect is neglected.
- Steam properties have been modelled with equivalent ideal gas properties based on IAPWS-97 formulation.

Table 1. CFD Model summary.

	Model Details
CFD Code	Fluent
Grid	Structured multi block
Turbulence model	Standard k-ε
Steam properties	Ideal gas
Flow	Steady flow
	Boundary conditions
Inlet	Total pressure - 5400 Pa Total temperature - 300 K Swirl angle and pitch angle - 0 degree Turbulence Intensity = 5%
Outlet	Static pressure - 4700 Pa
Wall	Adiabatic no slip wall
Other details	$Re = 2.8 \times 10^5$

3. Methodology

As stated in the previous section, this design optimization study is carried out in two phases. It may be noted that the last stage blade height is used as the reference dimension to present the length dimension. In the first phase, the end-wall distance (X), the casing outer diameter (D) and the volute section of the exhaust duct are considered. These three parameters define the geometrical envelope of the exhaust hood (Fig. 2). For the chosen diffusion ratio, the influence of the above parameters on the performance is studied. The exhaust hood geometries for the test cases were arrived at by varying one parameter at a time (X, D or volute profile).

The end-wall distance (X) is the distance of the end-wall from the inlet plane. An increase in the end-wall distance helps to increase the streamline length of flow

from the inlet to the outlet of the diffuser. As the increase in the streamline length reduces the adverse pressure gradient, it is expected to improve the performance of diffuser passage. On the other hand, the increased end-wall distance increases the distance between the bearings of the low-pressure turbine shaft, which is not a favourable condition from the perspective of turbine rotor dynamics. It is a challenge for design engineers as the knowledge on the impact of change in the end-wall distance on the exhaust hood performance is not available. The first three test cases are defined to study the effect of the end-wall distance on the exhaust hood performance. Considering the reference geometry as test Case C1, C2 is defined with reduced end-wall distance and C3 with increased end-wall distance.

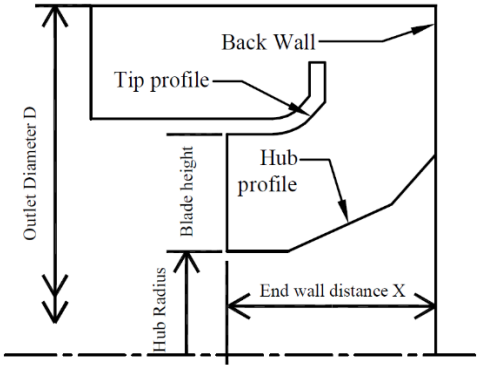

Fig. 2. Key geometry parameters of exhaust hood.

Next, the gap (*D1*) between the outlet of the diffuser to the casing at the top of the exhaust hood is considered. A reduction in the parameter *D1* means reduced area for the flow at the top of the exhaust hood, which results in increased flow resistance. On the other hand, a larger value of *D1* may result in a flow separation due to low momentum and sudden change in the flow direction. Hence, to study the impact of *D1*, test cases C4 and C5 with increased and reduced *D1* are constructed. Finally, the impact of volute design on the performance is considered. As the volute geometry eliminates the sudden expansion at the diffuser outlet, it is expected to reduce the total pressure loss in the exhaust hood. To study the significance of the volute geometry on the exhaust hood pressure loss, test cases C6 and C7 are defined with variable area guide vanes. It may be noted that the diffuser geometry is the same in both cases.

In the second phase, optimization of the multi-kink diffuser geometry is carried out. In the diffuser geometry (Fig. 3), areas *A1* - *A5* and the streamline lengths s1 - s4 are the possible design variables. The inlet area is defined by the last stage turbine blade height and hence it is not considered as a variable. Since the parametric study is conducted for a specific diffusion ratio, the outlet area (*A5*) is fixed. Hence, the actual independent variables are *A2*, *A3*, *A4*, *s1*, *s2*, *s3* and *s4*.

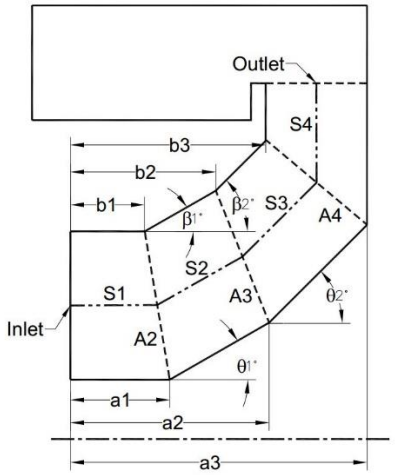

Fig. 3. Diffuser geometry definition.

As studied by Cao et al. [12], it is typical to conduct experiments by varying the design parameter in steps within a given range, to analyse the influence of a variable on the overall performance. In the above reference, the study is focussed on a flow guide tilt angle and observation is reported by calculating the change in static pressure recovery. However, this method of one variable at a time does not help to deduce any correlation between design variable and the performance and this method of experiments is limited mostly to a single variable situation. Cao et al. [13] extended their research to a multi factor optimization and considered four design parameters. Orthogonal experiment method is used to define the test cases as the variables are of YES or NO nature. In the present case, as the variables are not discrete but can assume any value within a given range and hence DOE is used to define the test cases. Use of DOE approach not only reduces the total number of experiments to be conducted but also provides a systematic means to study the interaction effects of the design variables [20].

As mentioned above, to define the test cases using DOE, the limit (minimum and maximum) values of each of the independent variable must be specified. However, the minimum and maximum limits of the intermittent areas (*A2*, *A3* and *A4*) are not known. Hence, the design procedure is updated to use the vertex coordinates of the diffuser, which in turn is used to calculate the intermittent areas. A multi-kink diffuser (Fig. 3) is defined with 10 vertex points. As the inlet location, inlet area, the outlet area and the end wall distance are specified, the four corner points of the diffuser geometry are fixed. Hence, the positions of the remaining 6 vertex are the variables.

Axial distance of each vertex is normalized with the end-wall distance. Along with normalized axial distance, angle at each vertex is considered as input variable to define the vertex location. The following rules are imposed in this new design procedure formulation.

- As the diffuser is axial-radial in nature, the initial segment of the diffuser shall be axial and the last segment shall be radial.

- Intermittent areas of the diffuser shall have incremental trend to ensure diffusion. ($A1 < A2 < A3 < A4 < A5$)
- The angle at each kink of the diffuser shall have increasing trend as the flow has to turn from horizontal to radial direction. ($\beta 1 < \beta 2$, $\theta 1 < \theta 2$, refer to Table 2)
- Axial distances of the tip curve and hub curve are normalized with their maximum distance and hence $b3^* = a3^* = 1$.

Table 2. List of diffuser geometry variables.

Variable	Range
$b1^*$	10 to 40 % of the total axial length
$b2^*$	10 to 50% of the total axial length
$\beta 1$	10^0 to 30^0
$\beta 2$	10^0 to 60^0, maximum of ($\beta 1$, 10)
$a1^*$	10 to 40 % of the total axial length
$a2^*$	of the total axial length
$\theta 1$	10^0 to 30^0
$\theta 2$	10^0 to 60^0, maximum of ($\theta 1$, 10)

After applying these constraints, there are 8 independent variables in the diffuser geometry design (Table 2). Taguchi's fractional factorial method is applied to define the test cases. Variables are listed as either maximum (MAX) or minimum (MIN). For each of the variable, the design range is arrived at based on the past design experience. For example, the design range for β1 is set as 10 to 30 degrees. As β1 is made with horizontal axis, less than 10 degrees results in insignificant area increase and more than 30 degrees will lead to a flow separation. Hence, the range is fixed as 10 to 30 degrees.

For each test case, the corresponding geometry is generated and the area variation from inlet to outlet is checked to ensure a continuously expanding flow area. For the defined test cases, CFD calculations are carried out and the results are presented in the next section.

Table 3. Geometrical variables summary for DOE.

	$b1^*$	$b2^*$	$\beta 1$	$\beta 2$	$a1^*$	$a2^*$	$\theta 1$	$\theta 2$
Case 1	MAX	MAX	MIN	MAX	MIN	MIN	MIN	MAX
Case 2	MAX	MAX	MAX	MAX	MAX	MAX	MAX	MIN
Case 3	MAX	MAX	MAX	MIN	MAX	MIN	MIN	MAX
Case 4	MIN	MAX	MAX	MAX	MIN	MIN	MAX	MIN
Case 5	MIN	MIN	MAX	MAX	MAX	MIN	MIN	MIN
Case 6	MIN	MIN	MAX	MIN	MAX	MAX	MAX	MAX
Case 7	MAX	MIN	MAX	MAX	MIN	MAX	MIN	MIN
Case 8	MAX	MIN	MAX	MIN	MIN	MIN	MAX	MAX
Case 9	MAX	MAX	MIN	MIN	MIN	MAX	MAX	MIN
Case 10	MIN	MIN	MIN	MIN	MIN	MIN	MIN	MIN
Case 11	MIN	MAX	MAX	MIN	MIN	MAX	MIN	MAX
Case 12	MIN	MIN	MIN	MAX	MIN	MAX	MAX	MAX
Case 13	MAX	MIN	MIN	MIN	MAX	MAX	MIN	MIN
Case 14	MAX	MIN	MIN	MAX	MAX	MIN	MAX	MAX
Case 15	MIN	MAX	MIN	MAX	MAX	MAX	MIN	MAX
Case 16	MIN	MAX	MIN	MIN	MAX	MIN	MAX	MIN

4. Results and Discussion

A minimum total pressure loss and a high degree of circumferential flow uniformity at the inlet plane are the key requirements of a good exhaust hood. Fig. 4 shows a comparison of the total pressure loss of all the cases in phase 1. From cases 1-3, it is concluded that the end-wall distance is not having a strong influence on the performance as the variation in pressure loss co-efficient (total pressure loss /inlet kinetic energy) due to change in the end-wall distance is less than 10%. Since a shorter end-wall distance is preferred for the rotor stability, an additional test case is attempted with further 10% reduced end-wall distance. However, it resulted in 30% increased total pressure loss. As discussed earlier, reduction in end-wall distance leads to reduced length of flow. In other words, for the same diffuser area ratio, reduction in the end-wall distance reduces the flow travel length and hence increases the rate of diffusion (increase in area per unit length of diffuser). Hence, it is concluded that a further reduction in the end-wall distance is not recommended. From the results of Cases 4 and 5, it is obvious that the gap between the diffuser outlet and the outer casing plays a critical role in the exhaust hood performance. Increase of the gap to 50% of the blade height (from the base case of 25%) resulted in 26% reduction in pressure loss. The peak flow velocity at the diffuser outlet region became smaller with increase in the gap. As the larger gap resulted in reduced pressure loss, one additional case was attempted with further increasing the gap to 70% of the blade height (not shown in the figure). With increased gap, the size of recirculation region increased and hence no further reduction in pressure loss occurred. Cases 6 and 7, which correspond to the volute shape design changes and resulted in higher pressure losses. Hence, it is considered that volute shape does not have a strong influence on the exhaust hood performance. It may be noted that the volute geometry can guide the flow only beyond the outlet of the diffuser.

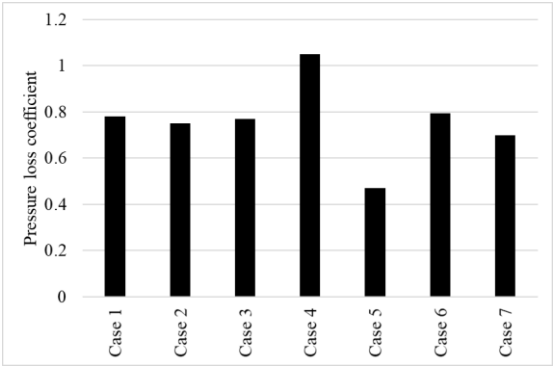

Fig. 4. Pressure loss comparison.

As major portion of the pressure loss occurs in the diffuser passage where the flow velocity is high, it is concluded that the volute design is not having a strong influence on the overall performance. Hence, from the above analysis of phase 1 variables, within the design range considered, the diffuser gap is the most affecting parameter on the pressure loss and a diffuser gap of about 50% blade height is found to be beneficial.

To quantify the influence of the end-wall position on the performance, a study is performed. Geometries are defined with end-wall distance of 1.5, 1.9 and 2.5 and other diffuser geometry variables as per Case 6 of Table 3. Figure 5 shows that a significant improvement in performance is possible for the normalized end distance up to the 1.9. However, any further increase in normalized end-wall distance beyond 1.9 did not produce an increase in the mass flow rate. Further, from the study of the velocity profile at the inlet (Fig. 6) a good performing diffuser has a higher velocity at the inlet. In addition, the rate of increase in velocity from the hub to the tip is steeper for high performing design.

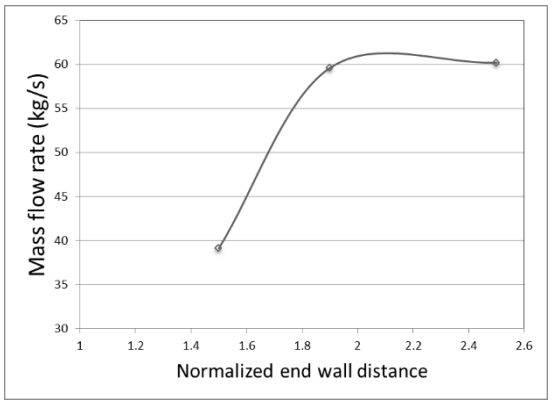

Fig. 5. Variation of mass flow rate with end-wall distance.

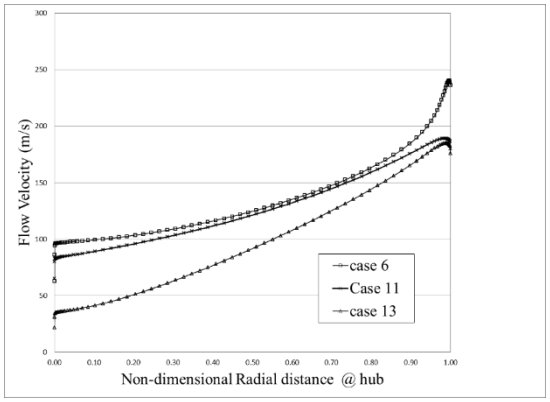

Fig. 6. Inlet velocity profile.

As mentioned in the methodology section, Phase 2 studies are conducted to investigate the influence of the diffuser geometrical parameters on the performance. The geometries are configured as per the values of the variables specified in Table 3. For each design, CFD analysis is carried out with total pressure inlet and static pressure outlet conditions.

The flow behaviours of all the cases have been presented in Fig. 7. It can be observed that Cases 1, 4, 5, 14 and 15 have a flow separation on the hub surface. These flow separations are local in nature as they can be found reattached to the hub surface at some downstream point. A possible explanation for this behaviour is that

the axial momentum tends to push the flow towards the wall. On the other hand, in Cases 4, 7 and 8 it can be observed that the flow separations, which begins at the tip continues to remain till the outlet. Hence, the losses due to hub separation is less significant. In geometries 2, 3, 8 and 13, hub surface has steep angles of $\theta 1$ and $\theta 2$, which resulted in increased losses due to the local acceleration in the diffuser. Hence, it is concluded that the tip profile is having a stronger influence on the diffuser performance when compared to the hub profile. Hence, it is recommended to focus on the tip surface related variables for optimizing the performance.

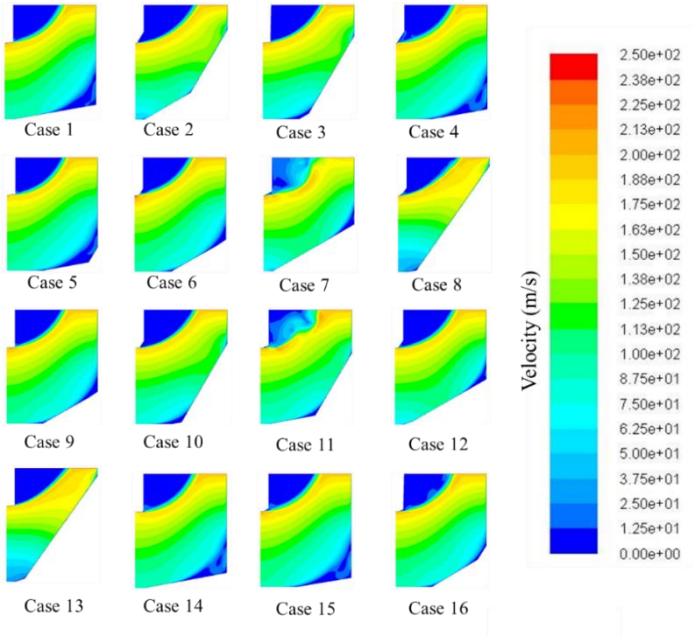

Fig. 7. Velocity contour plot of DOE test cases.

The streamline curvature length of the diffuser is different for each design as it changes with the geometrical parameters. The combination of maximum $b1^*$ and minimum $\beta 1$ gives a longer tip curve length. It is observed that the combinations, in which, $b1^*$ is maximum and $\beta 1$ is minimum, (cases 1, 9 and 14) lead to a straight section of axial flow followed by a radial flow passage. As a little or no diffusion is expected in the axial flow portion of the diffuser, the effective diffuser length is smaller than the total streamline curvature length. Cases 1 and 9, which are with maximum $b1^*$ and minimum $\beta 1$ have a large flow separation at the tip region. Hence, these cases have lesser mass flow rates. Cases 4 and 6 have the combination of minimum $b1^*$ and maximum $\beta 1$. These cases have diffusion from the inlet plane and hence a longer diffuser.

From Fig. 8, it can be observed that the performance of these cases is good. Compared to Case 4, Case 6 has a higher performance, which can be attributed to its better hub surface design. Case 4 has an L shaped hub surface, which resulted in a stagnation zone, which is avoided in Case 6. Case 13 has the combination of minimum tip angles ($\beta 1$ and $\beta 2$) and maximum hub angles ($\theta 1$ and $\theta 2$) resulted in accelerated flow regions and also a large separation due to sudden change in flow direction. Due to these adverse conditions, Case 13 has the lowest mass flow rate.

Further analysis of results from Fig. 8 shows that Cases 2 and 8, which have maximum hub angle ($\theta 1$, $\theta 2$) also produce lower performance as increased hub angle reduces the geometrical diffusion ration. From these results it can be concluded that Case 6 has the optimum parameters.

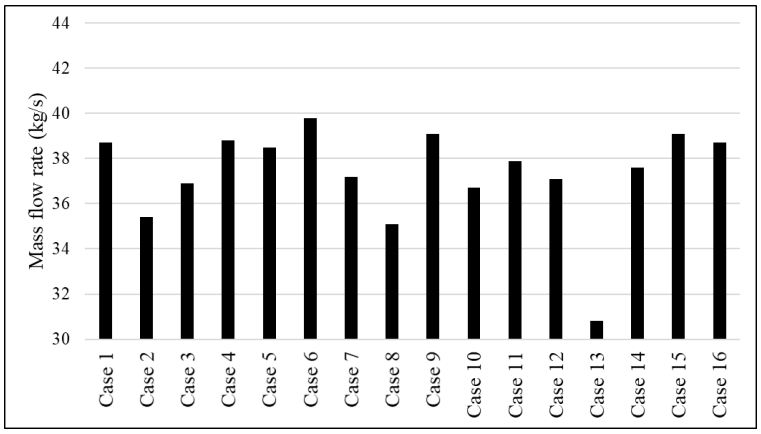

Fig. 8. Predicted mass flow rates.

5. Conclusions

Sensitivity analysis of the parameters, which define the outer envelope and design optimization of a multi-kink axial radial diffuser have been carried out. A minimum non-dimensionalized end-wall distance of 1.9 is recommended since a further reduction of the end-wall distance results in a flow separation in the diffuser passage leading to a significant pressure loss. The gap between the outlet of the diffuser to the exhaust hood outer casing is found to be significantly influencing the flow in the diffuser passage producing an optimum performance at 50% of the last stage blade height. Another important conclusion emerged from this study is that the tip profile is more influencing the performance than the hub surface. From the DOE, a right combination of diffuser tip geometrical parameters producing a higher stream length results in elimination of flow separation and thus an enhanced performance.

Nomenclatures

D	Casing outer diameter, m
$D1$	Minimum gap between the casing outer diameter to the tip of the diffuser, m
L	Length of the last stage blade, m
P	Pressure, Pa
U	Velocity, m/s

Greek Symbols

ρ	Density, kg/m^3
β, θ^*	Angles on the tip and hub surfaces respectively denotes non-dimensional distance

References

1. Burton, Z.; Ingram, G.L.; and Hogg, S. (2013). A literature review of low pressure steam turbine exhaust hood and diffuser studies. *Journal of Engineering for Gas Turbines and Power*, 135(6), 10 pages.
2. Tindell, R.H.; Alston, T.M.; Sarro, C.A.; Stegmann, G.C.; Gray, L.; and Davids, J. (1996). Computational fluid dynamics analysis of a steam power plant low pressure turbine downward exhaust hood. *Journal of Engineering for Gas Turbines and Power*, 118(1), 214-224.
3. Veerabathraswamy, K.; and Kumar, A.S. (2016). Effective boundary conditions and turbulence modeling for the analysis of steam turbine exhaust hood. *Applied Thermal Engineering*, 103, 773-780.
4. Fu, J.; Liu, J.; and Zhou, S. (2007). Experimental and numerical investigation of interaction between turbine stage and exhaust hood. *Proceedings of the Institution of Mechanical Engineers, Part A*, 221(7), 991-999.
5. Liu, J.J.; Cui, Y.Q.; and Jiang, H.D. (2003). Investigation of flow in a steam turbine exhaust hood with/without turbine exit conditions simulated. *Journal of Engineering for Gas Turbines and Power*, 125(1), 292-299.
6. Benim, A.C.; Geiger, M.; Doehler, S.; Schoenenberger, M.; and Roemer, H. (1995). Modelling the flow in the exhaust hood steam turbines under consideration of the turbine-exhaust hood interaction. *Proceedings of the First European Conference on Turbomachinery-Fluid Dynamic and Thermodynamic Aspects.* Erlangen, Germany, 343-357.
7. Wang, H.; Zhu, X.; and Du, Z. (2010). Aerodynamic optimization for low pressure turbine exhaust hood using Kriging surrogate model. *International Communications in Heat and Mass Transfer*, 37(8), 998-1003.
8. Ris, V.V.; Simoyu, L.L.; Galaev, S.A.; Gudkov, N.N.; Kirillov, V.I.; Smirnov, M.; Kirillov, A.I.; and Ermolaev, V.V. (2009). Numerical Simulation of flow in a steam turbine exhaust hood: Comparison results of calculations and data from a full scale experiment. *Thermal Engineering*, 56(4), 277-283.
9. Fan, T.; Xie, Y.; Zhang, D.; and Sun, B. (2007). A combined numerical model and optimization for low pressure exhaust system in steam turbine. *Proceedings of ASME Power Conference.* San Antonio, Texas, 349-358.
10. Cao, W.-x.; and You, X.-y. (2017). The inverse optimization of exhaust hood by using intelligent algorithms and CFD simulation. *Powder Technology*, 315, 282-289.
11. Gardzilewicz, A.; Swirydczuk, J.; Badur, J.; Karcz, M.; Werner R.; and Szyrejko, C. (2003). Methodology of CFD computations applied for analyzing flows through steam turbine exhaust hoods. *Transactions of the Institute of Fluid-Flow Machinery*, 113, 157-168.
12. Cao, L.; Lin, A.; Li. Y.; and Xiao, B. (2017). Optimum tilt angle of flow guide in steam turbine exhaust hood considering the effect of last stage flow field. *Chinese Journal of Mechanical Engineering*, 30(4), 866-875.
13. Cao, L.; Si, H.; Lin, A.; Li, P.; and Li, Y. (2017). Multi-factor optimization study on aerodynamic performance of low-pressure exhaust passage in steam turbines. *Applied Thermal Engineering*, 124, 224-231.

14. Verstraete, T.; Prinsier, J.; Sante, A.D.; Gatta, S.D.; and Cosi, L. (2012). Design optimization of a low pressure steam turbine radial diffuser using an evolutionary algorithm and 3D CFD. *Proceedings of the Turbine Technical Conference and Exposition.* Volume 6: Oil and Gas Applications, Concentrating Solar Power Plants, Steam Turbines, Wind Energy. Copenhagen, Denmark, 603-613.
15. Fu, J.-L.; Liu, J.-J. and Zhou, S.-J.; (2014). Aerodynamic optimization of the diffuser towards improving the performance of turbine and exhaust hood. Volume IB: Marine, Microturbines, Turbocharges and small Turbomachines, Steam Turbines. *Proceedings of the Turbine Technical Conference and Exposition*. Dusseldorf, Germany, 10 pages.
16. Yoon, S.; Stanislaus, F.J.; Mokulys, T.; Singh, G.; and Claridge, M. (2011). A three dimensional diffuser design for the retrofit of a low pressure turbine using in-house exhaust design system. *Proceedings of the Turbine Technical Conference and Exposition.* Volume 7: Turbomachinery, Parts A, B and C. Vancouver, British Columbia, Canada, 2309-2319.
17. Menter, F.R.; Kuntz, M.; and Langtry, R. (2003). Ten years of industrial experience with the SST turbulence model. *Turbulence, Heat and Mass Transfer* 4, 8 pages.
18. Senoo, S.; Takahashi, F.; Shikano, Y.; and Kimura, T. (2004). The computational technique for compressible fluid based on steam properties and performance improvements on steam turbines. *Proceedings of the 14th International Conference on the Properties of Water and Steam*. Kyoto, Japan, 655-659.
19. Patankar, S.V. (1980). *Numerical heat transfer and fluid flow*. Washington, United States of America: Hemisphere Publishing Corporation.
20. Oehlert, G.W. (2000). *A first course in design and analysis of experiments*. New York, United States of America: W. H. Freeman and Company.